GEODYNAMIC SIGNIFICANCE OF THE JANATABAD PERIDOTITES AND ASSOCIATED CHROMITITES (S IRAN): IMPLICATIONS FOR SUBDUCTION INITIATION

Reza Monsef*,✉, Iman Monsef** and **Mohammad Rahgoshay*****

* *Department of Geology, Estahban branch, Islamic Azad University, Estahban, Iran.*
** *Department of Earth Sciences, Institute for Advanced Studies in Basic Sciences (IASBS), Zanjan, Iran.*
*** *Faculty of Earth Sciences, Shahid Beheshti University, Tehran, Iran.*
✉ *Corresponding author, email: iman_monsef@yahoo.com*

Keywords: *Janatabad peridotites, chromitites, subduction initiation, Neo-Tethys. Southern Iran.*

ABSTRACT

The Janatabad peridotites are exposed in the Hajiabad-Esfandagheh Mélange Zone in the southern part of Iran. These peridotites are dominantly composed of harzburgites with small lenses and veins of chromitite ores surrounded by dunite sheaths. Harzburgites have accessory chromites characterized by moderate X_{Cr} of 0.59-0.61, and X_{Mg} of 0.52-0.58, resembling depleted mid-ocean ridge peridotites, supposed to have originated as the residue from a high degree of partial melting and MORB-like magma extraction at the inception of subduction. Dunites can be divided into two types: Type 1 dunite with moderate X_{Cr} of 0.53-0.62 and X_{Mg} of 0.48-0.53, and Type 2 dunite with high X_{Cr} of 0.63-0.67 and low X_{Mg} of 0.40-0.48. Two distinctive melts are required for the formation of these dunites: a MORB-like melt for the Type 1 dunite, and a transitional-like melt for the Type 2 dunite. These compositional variations from MORB to melts transitional between MORB and boninite are due to the hydrous fluids derived from the subducted oceanic slab into the overlying mantle wedge at the beginning of the down dip motion of the slab. Al-rich podiform chromitites, characterized by relatively low X_{Cr} of 0.53-0.54 and relatively high X_{Mg} of 0.60-0.71, may have formed from MORB-like melts.

In particular, the interaction between primitive MORB-like melts and depleted harzburgites produced Type 1 dunites and secondary silica-rich melts from which Al-rich chromitites crystallized. Type 2 dunites can be generated by the interaction between transitional-like melts and depleted harzburgites above a lithosphere in subsidence. Accordingly, it is inferred that the Janatabad peridotites formed by rifting of a Late Triassic to Early Jurassic embryonic ocean during subduction initiation of Neo-Tethyan lithosphere in an intra-oceanic environment.

INTRODUCTION

The Neo-Tethyan domain in Iran was created by extension of oceanic lithosphere between the Central Iranian Block and the Arabian Plate during Late Permian time (Berberian and King, 1981). Subduction of the Neo-Tethyan Ocean started during Late Triassic-Early Jurassic time in an arc-related tectonic environment. Subduction led to volcanic activity and emplacement of intrusive bodies within two parallel subduction-related magmatic belts, i.e. the Mesozoic Sanandaj-Sirjan and Cenozoic Urumiyeh-Dokhtar Magmatic Arcs (Fig. 1a). The arc magmatism was followed by marginal basin spreading which occurred from Late Triassic to Late Cretaceous (e.g., Hajiabad-Esfandagheh Mélange Zone) or Late Cretaceous (e.g., Shahr-e-Babak-Baft Mélange Zone) in the Central Iranian Block (Fig. 1a). All data on the ophiolitic complexes in these regions confirm the presence of multi-branched transtensional marginal basins along the active margin of the Central Iranian Block (Ghasemi et al., 2002; Ahmadipour et al., 2003). The marginal basin system collided with the Arabian passive margin in the Late Cretaceous along the NW-SE trending Main Zagros Thrust Belt.

The Janatabad peridotites are exposed in the Hajiabad-Esfandagheh Mélange Zone in the southern part of Iran. These peridotites mainly consist of harzburgites enclosing dunites and associated chromitites. Peridotites record a spinel-peridotite facies condition, and a deformation history yielding tectonite to mylonite fabrics.

Peridotites from subduction-related environments can provide important information on melt generation and melt-mantle interaction above subduction zone systems (Pearce et al., 2000). Chromitites formed in mantle peridotites in various tectonic environments have compositional differences and hence provide a powerful indicator to determine their petrogenetic and geotectonic setting (Dick and Bullen, 1984; Barnes and Roeder, 2001; Kamenetsky et al., 2001; Arai et al., 2006).

This article evaluates the geodynamic significance of the Janatabad peridotites and associated chromitites in the southern part of Iran. In this contribution, we present for the first time geology, petrography and mineral chemistry of the Janatabad peridotites, in order to elucidate their tectonic setting.

GEOLOGICAL SETTING

The Janatabad region lies in the Hajiabad-Esfandagheh Mélange Zone and consists of Eocene and Creaceous flysch type sediments, and a Late Triassic to Late Cretaceous mélange associated with Late Triassic to Early Jurassic peridotite bodies (Azizan and Nazemzadeh, 2006) (Fig. 1b, c).

The mélange defines a NW-SE oriented belt and consists of peridotites, meta-volcanics and pelagic limestones. The contact between mélange and peridotites is interpreted as a thrust fault. Also, the Eocene flysch-type sediments are found within the mélange. The meta-volcanics mainly consist of meta-pyroclastics, meta-basalts and meta-andesites. The mélange is unconformable overlain by younger flysch-type sediments.

The peridotites occur as isolated bodies within the mélange. They are generally massive and become foliated along the shear zones. Geological investigation indicates that the peridotites are bounded by thrust faults suggesting a tectonic emplacement.

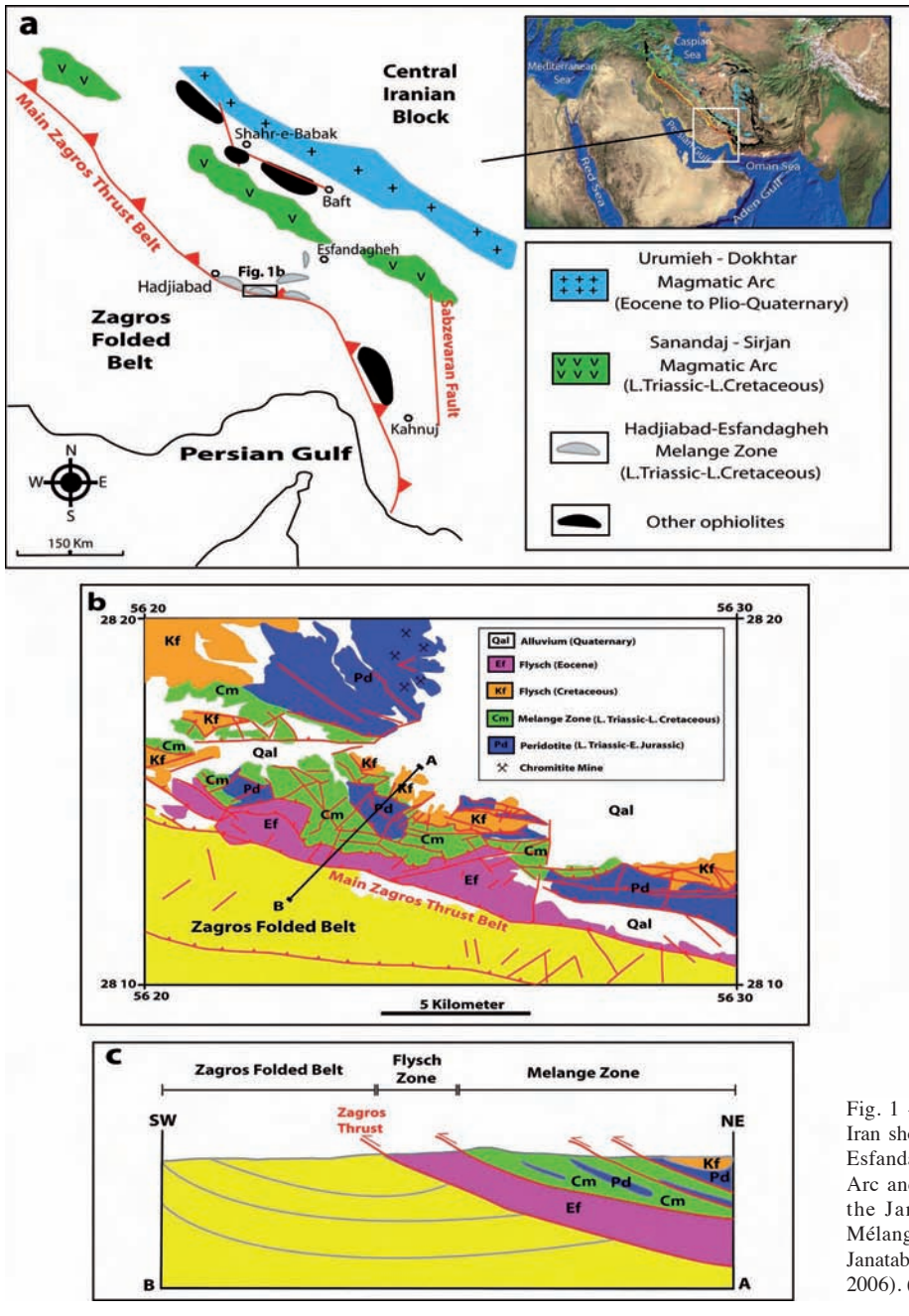

Fig. 1 - (a) Tectonic sketch map of the southern part of Iran showing the distribution and extent of the Hajiabad-Esfandagheh Mélange Zone, Sanandaj-Sirjan Magmatic Arc and Urumiyeh-Dokhtar Magmatic Arc. Location of the Janatabad region in the Hajiabad-Esfandagheh Mélange Zone is illustrated. (b) Geological map of the Janatabad region (modified after Azizan and Nazemzadeh, 2006). (c) Schematic cross-section of the Janatabad region.

Mantle rocks include harzburgites, dunites and serpentinites. Significant chromitite ore bodies occur as lens- and vein-shaped masses of podiform type within the mantle peridotites. Host harzburgites form the major constituents of the Janatabad peridotites, whereas chromitites are found as minor constituents and are invariably surrounded by dunite envelopes (Fig. 2a). Dunites with different types of chromites occur close to each other, and the boundaries between dunite envelopes and harzburgites are relatively sharp (Fig. 2b).

The podiform chromitite bodies and their dunite envelopes are typically sub-concordant with respect to the tectonite foliation. Chromitite lenses show a NW-SE orientation conformable with the regional structure. The chromitite ore bodies range in texture from massive to disseminated types from the center of the ore bodies to the edges.

PETROGRAPHY

Harzburgite

The most common texture in the harzburgites is porphyroclastic; it is characterized by medium-grained (1-2 mm) subhedral crystals of orthopyroxene and olivine with minor chromite and clinopyroxene (rarely exceeding 5 vol.%) (Fig. 3a). These minerals show evidence of deformation such as subgrain structure, kink banding and undulose extinction. Subgrain structure and undulose extinction are developed in olivine. Grain shapes are irregular for orthopyroxene and olivine porphyroclasts. Orthopyroxene porphyroclasts are bent and occasionally kink banding is developed. In the harzburgites samples, chromite occur as vermicular grains at the margins of olivine (Fig. 3a). The disseminated chromite is typically less than 1 vol.%.

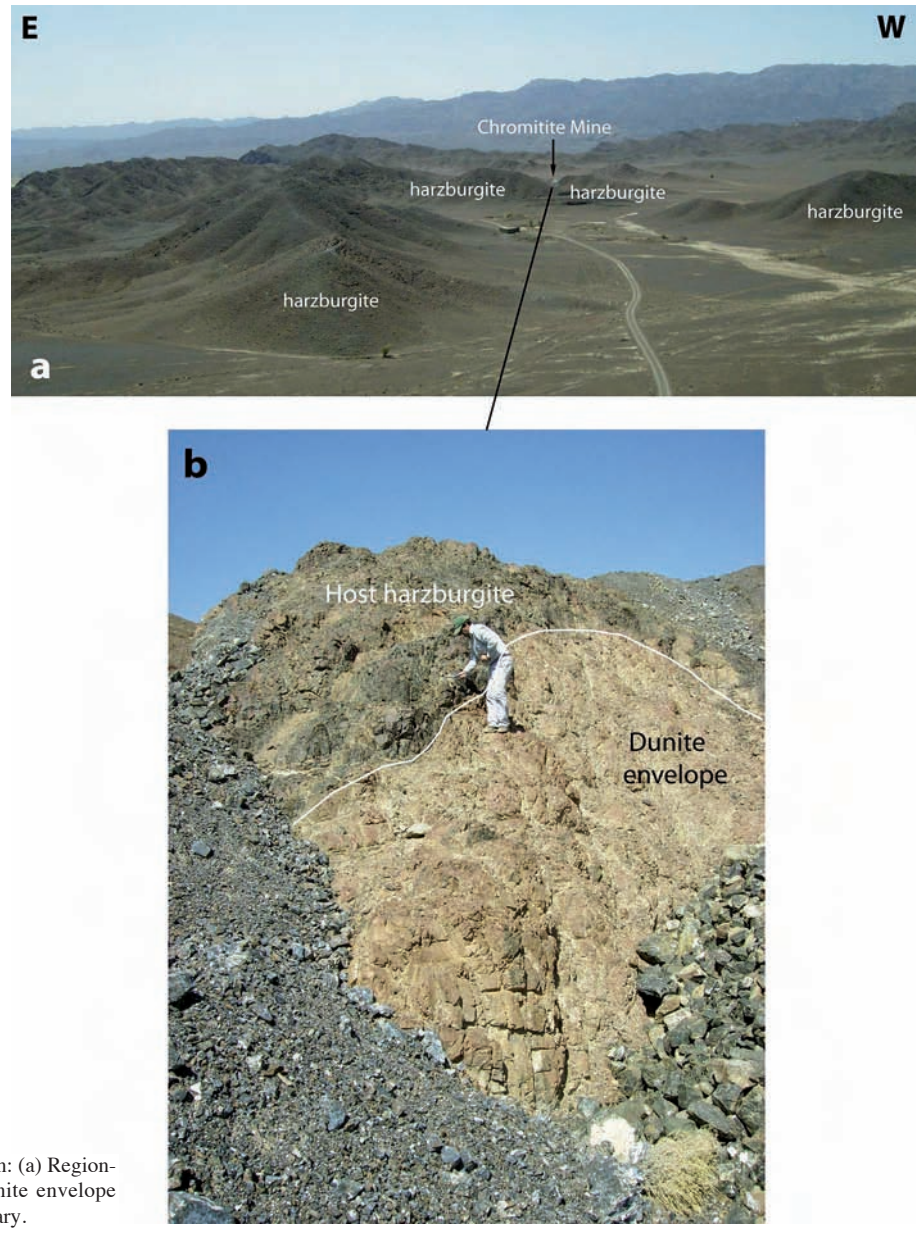

Fig. 2 - Field photographs from the Janatabad region: (a) Regional overview of the Janatabad peridotites. (b) Dunite envelope within host harzburgite with relatively sharp boundary.

Dunite

Dunites essentially consist of olivine (partially to extensively replaced by serpentine minerals) and chromite. Equigranular and porphyroclastic textures are the most common textures (Fig. 3b). Subgrain structure and undulatory extinction are ubiquitous in olivine. Grain size of the olivine porphyroclasts is variable, and typically ranges from 1 to 2 mm. Recrystallization and neoblasts of olivine are not observed. The disseminated chromite in dunite occurs either as euhedral to subhedral crystals with grain size of about 0.1 mm either as droplets in olivine (Fig. 3b).

Serpentinite

Serpentinites are dominantly composed of serpentine with variable amounts of chromite, talc and chlorite (Fig. 3c). Serpentinite preserves pseudomorphs of olivine indicating that the protolith was dunitic. Chlorite shows cross fiber veinlets in a serpentine matrix and mesh texture indicating that it formed after serpentinization. The disseminated opaque minerals in the serpentinites are chromite droplets (Fig. 3c). Chromite grains also form small (0.05 to 0.1 mm in size) euhedral to subhedral crystals which typically occur between the serpentine minerals.

Chromitite

Disseminated ore is one of the most commonly encountered types of chromitite in the study area. Chromitite pods consist mostly of 40-70 vol.% of subhedral to anhedral chromite crystals in a meshwork matrix of secondary serpentine and olivine grains (Fig. 3d). Aggregates of chromite grains generally range from 1-2 mm in size.

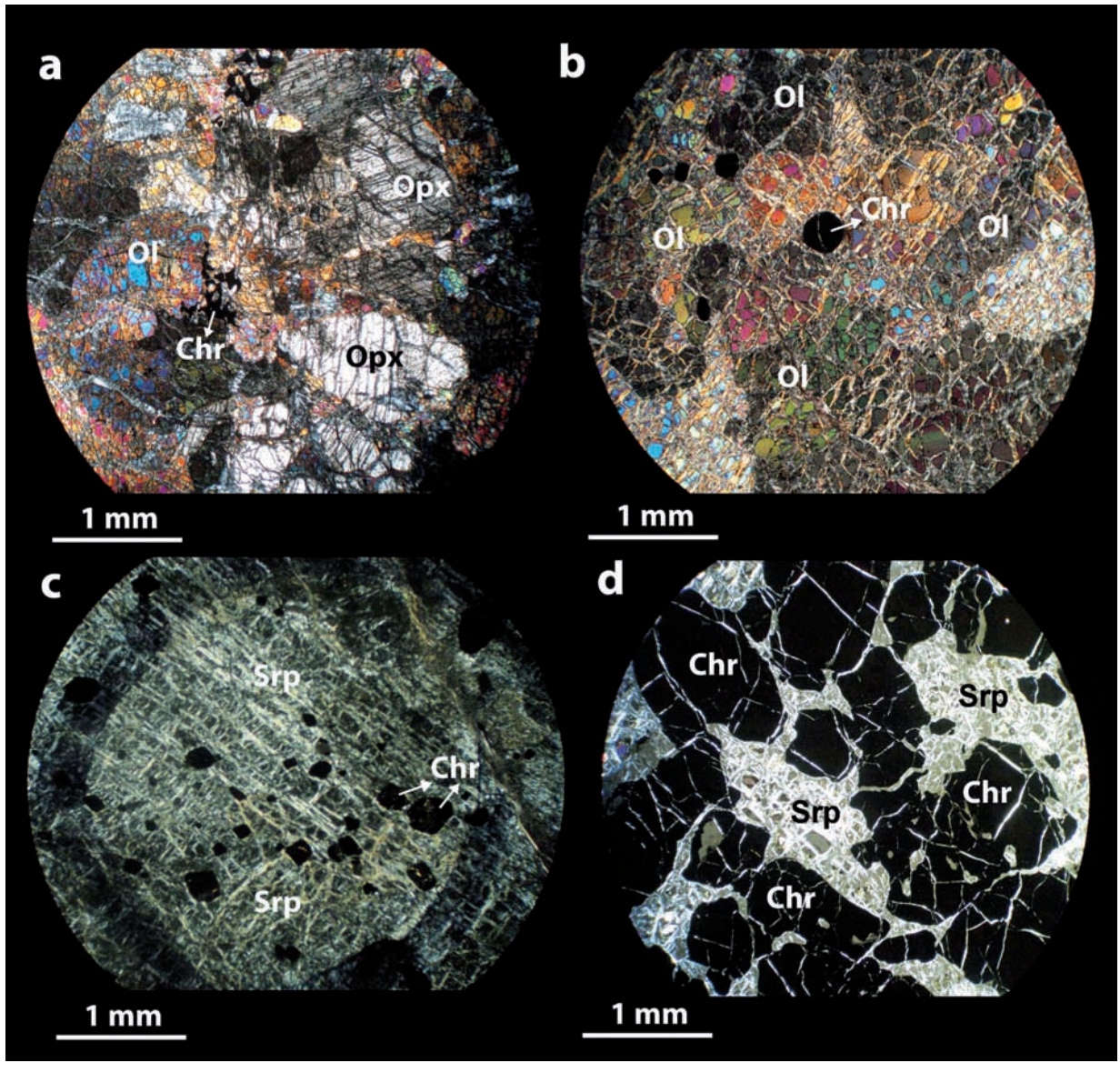

Fig. 3 - Photomicrographs of peridotite and chromitite samples, all taken with crossed polarizers. Opx- orthopyroxene; Ol- olivine; Chr- chromite; Srp- serpentine. (a) Harzburgite with porphyroclastic texture. Vermicular chromite occurs in olivine (JT07-3); (b) Dunite with elongate porphyroclastic textures. Chromite grains occur in olivine (JT07-1); (c) Serpentinite. The disseminated chromites occur between the serpentine minerals (JT07-12); (d) Chromitite with chromite aggregates in a matrix of secondary serpentine and olivine relicts (JT07-8).

MINERAL CHEMISTRY

Analytical methods

The compositions of minerals in peridotites and associated chromitites were determined by electron microprobe analyses (EPMA of CAMECA SX-100 model) with a wavelength dispersive analyser system at the microprobe lab Camparis, Paris VI University (Campus Jussieu), France. Natural silicate minerals and suitable synthetic oxides were used for calibration.

For this purpose, all analyses were performed with an accelerating voltage of 15 keV, and a focused electron beam with 10 nA current. Major element concentrations and end member compositions of olivine, orthopyroxene and chromite in harzburgites, dunites and chromitites are listed in tables 1, 2 and 3 respectively.

Olivine

The forsterite [Fo = 100 Mg/ (Mg + Fe^{2+})] contents of olivine vary from Fo_{91} to $Fo_{91.4}$ in harzburgites and from $Fo_{90.1}$ to $Fo_{93.2}$ in dunites (Fig. 4a, b). The NiO contents of olivine range from 0.29 to 0.43 wt% in harzburgites and from 0.26 to 0.48 wt% in dunites. The NiO and Fo contents of olivine do not display systematic variations between harzburgites and dunites (Fig. 4a).

Table 1 - Compositions of olivine in harzburgites and dunites from the Janatabad peridotites.

Sample Rock	JT07-3 Harzburgite	JT07-3 Harzburgite	JT07-4 Harzburgite	JT07-4 Harzburgite	JT07-4 Harzburgite	JT07-1 Dunite	JT07-1 Dunite	JT07-1 Dunite	JT07-1 Dunite
SiO_2	40.87	40.50	40.97	40.58	40.91	40.24	40.11	40.71	40.54
TiO_2	0.02	0.02	0.01	0.03	0.01	0.02	0.05	0.06	0.05
Al_2O_3	0.01	0.01	0.02	0.02	0.00	0.01	0.02	0.00	0.01
Cr_2O_3	0.04	0.01	0.04	0.08	0.02	0.07	0.01	0.04	0.08
FeO	8.72	8.93	8.60	8.47	8.87	8.72	8.86	9.31	9.26
MnO	0.14	0.12	0.22	0.12	0.14	0.15	0.15	0.18	0.23
MgO	50.89	50.95	50.59	50.62	50.67	50.74	50.64	50.77	51.03
NiO	0.32	0.35	0.43	0.41	0.29	0.31	0.44	0.47	0.41
CaO	0.00	0.04	0.02	0.01	0.05	0.02	0.00	0.03	0.03
Total	101.00	100.94	100.90	100.32	100.95	100.28	100.28	101.56	101.63
Si	0.989	0.983	0.992	0.988	0.991	0.982	0.980	0.984	0.979
Ti	0.000	0.000	0.000	0.000	0.000	0.000	0.001	0.001	0.001
Al	0.000	0.000	0.000	0.000	0.000	0.000	0.001	0.000	0.000
Cr	0.001	0.000	0.001	0.001	0.000	0.001	0.000	0.001	0.001
Fe	0.176	0.181	0.174	0.172	0.180	0.178	0.181	0.188	0.187
Mn	0.003	0.003	0.004	0.002	0.003	0.003	0.003	0.004	0.005
Mg	1.835	1.843	1.826	1.837	1.829	1.846	1.844	1.829	1.837
Ni	0.006	0.007	0.008	0.008	0.006	0.006	0.009	0.009	0.008
Ca	0.000	0.001	0.000	0.000	0.001	0.000	0.000	0.001	0.001
Fo	91.2	91.1	91.3	91.4	91.1	91.2	91.1	90.7	90.8

Sample Rock	JT07-2 Dunite	JT07-2 Dunite	JT07-2 Dunite	JT07-2 Dunite	JT07-2 Dunite	JT07-5 Dunite	JT07-5 Dunite	JT07-6 Dunite	JT07-6 Dunite	JT07-6 Dunite	JT07-6 Dunite	JT07-6 Dunite	JT07-7- Dunite
SiO_2	40.35	40.75	40.15	40.10	39.80	41.50	41.76	41.42	41.23	40.90	41.71	41.82	40.86
TiO_2	0.06	0.04	0.05	0.07	0.03	0.00	0.05	0.01	0.03	0.01	0.01	0.00	0.00
Al_2O_3	0.01	0.01	0.03	0.01	0.02	0.00	0.00	0.01	0.00	0.00	0.00	0.00	0.02
Cr_2O_3	0.05	0.04	0.01	0.02	0.09	0.00	0.00	0.00	0.00	0.00	0.07	0.03	0.00
FeO	8.89	9.16	9.04	9.39	8.97	6.52	6.67	8.88	9.38	9.34	9.55	9.36	7.21
MnO	0.09	0.05	0.09	0.20	0.15	0.17	0.07	0.17	0.20	0.13	0.14	0.16	0.10
MgO	50.96	51.02	50.65	50.99	50.61	50.50	51.23	48.98	48.70	48.02	48.85	49.11	50.63
NiO	0.40	0.31	0.37	0.45	0.38	0.36	0.30	0.34	0.45	0.29	0.33	0.31	0.30
CaO	0.01	0.02	0.03	0.02	0.05	0.03	0.05	0.07	0.10	0.06	0.08	0.10	0.07
Total	100.82	101.39	100.42	101.25	100.09	99.07	100.13	99.87	100.09	98.74	100.74	100.90	99.18
Si	0.980	0.984	0.980	0.974	0.976	1.011	1.007	1.012	1.009	1.013	1.013	1.013	0.999
Ti	0.001	0.001	0.001	0.001	0.001	0.000	0.001	0.000	0.001	0.000	0.000	0.000	0.000
Al	0.000	0.000	0.001	0.000	0.000	0.000	0.000	0.000	0.000	0.000	0.000	0.000	0.001
Cr	0.001	0.001	0.000	0.000	0.002	0.000	0.000	0.000	0.000	0.000	0.001	0.001	0.000
Fe	0.181	0.185	0.184	0.191	0.184	0.133	0.135	0.181	0.192	0.193	0.194	0.190	0.147
Mn	0.002	0.001	0.002	0.004	0.003	0.003	0.001	0.003	0.004	0.003	0.003	0.003	0.002
Mg	1.845	1.837	1.843	1.845	1.849	1.834	1.842	1.784	1.776	1.773	1.768	1.774	1.846
Ni	0.008	0.006	0.007	0.009	0.007	0.007	0.006	0.007	0.009	0.006	0.006	0.006	0.006
Ca	0.000	0.001	0.001	0.000	0.001	0.001	0.001	0.002	0.003	0.002	0.002	0.003	0.002
Fo	91.1	90.9	90.9	90.6	91.0	93.3	93.2	90.8	90.3	90.2	90.1	90.3	92.6

See text for analytical details. Atomic proportions have been calculated on the basis of 4 oxygens.

Orthopyroxene

The orthopyroxenes from harzburgites are mostly Mg-rich enstatite in composition. The Mg-number [X_{Mg} = Mg / (Mg + Fe^{total}) atomic ratio] of orthopyroxene varies from 0.91 to 0.92. Al_2O_3 contents are low (1.44 - 1.61 wt%, Fig. 5). They show a narrow compositional range of TiO_2 (0.02-0.12 wt%), Cr2O3 (0.48-0.63 wt%), MgO (35.40-35.79 wt%) and CaO (0.45-0.72 wt%).

Chromite

The Cr-number [X_{Cr}= Cr/ (Cr + Al) atomic ratio] ranges from 0.53 to 0.54 in chromitites, 0.59 to 0.61 in harzburgites and 0.58 to 0.67 in dunites. Based on the Cr-number of chromites, the dunites can be classified into two types: Type 1 dunite, with Cr-number of 0.58-0.62 (JT07-2 and JT07-5 samples), and Type 2 dunite, with Cr-number of 0.63-0.67 (JT07-1, JT07-6 and JT07-7 samples). The Mg-number [X_{Mg} = Mg/ (Mg + Fe^{2+}) atomic ratio] varies between 0.60 to 0.71 in chromitites, 0.52 to 0.58 in harzburgites, 0.48 to 0.53 in Type 1 dunites, and 0.40 to 0.48 in Type 2 dunites (Fig. 6a).

TiO_2 contents vary between 0.16 and 0.38 wt%, typical of ophiolitic chromites. Note that a few chromites show a weak enrichment in TiO_2. There is a broader range of TiO_2 contents in chromites from dunites and harzburgites and a narrower range of TiO_2 contents in chromites from chromitites (Fig. 6b).

Chromites in the chromitites have higher Al_2O_3 contents (24.0-25.5 wt%) relative to chromites in dunites (15.1-21.9 wt%) and harzburgites (20.9-21.3 wt%). Cr_2O_3 concentrations are higher in harzburgites (46.6-48.2 wt%) and dunites (42.8-46.8 wt%) with respect to those in chromitites (41.6-42.8 wt%). The amount of MgO is maximum in chromites from chromitites (12.7-15.7 wt%), followed by harzburgites (11.0-12.4 wt%) and dunites (7.88-11.3 wt%).

Table 2 - Compositions of orthopyroxene in harzburgites from the Janatabad peridotites.

Sample Rock	JT07-3 Harzburgite	JT07-3 Harzburgite	JT07-4 Harzburgite	JT07-4 Harzburgite	JT07-4 Harzburgite
SiO_2	55.71	55.84	55.82	56.71	57.04
TiO_2	0.12	0.03	0.03	0.09	0.02
Al_2O_3	1.44	1.57	1.49	1.61	1.53
Cr_2O_3	0.63	0.53	0.53	0.48	0.59
Fe_2O_3	4.16	3.95	4.31	3.18	1.95
FeO	2.12	2.31	2.04	3.08	4.05
MnO	0.23	0.24	0.12	0.10	0.11
MgO	35.76	35.55	35.79	35.70	35.40
CaO	0.45	0.62	0.55	0.70	0.72
Na_2O	0.01	0.01	0.01	0.02	0.01
K_2O	0.01	0.00	0.03	0.03	0.00
Total	100.63	100.65	100.71	101.68	101.41
Si	1.923	1.927	1.925	1.933	1.944
Ti	0.003	0.001	0.001	0.002	0.000
Al	0.058	0.064	0.060	0.065	0.061
Cr	0.017	0.014	0.014	0.013	0.016
Fe	0.168	0.168	0.169	0.168	0.165
Mn	0.007	0.007	0.003	0.003	0.003
Mg	1.841	1.828	1.840	1.814	1.799
Ca	0.017	0.023	0.020	0.025	0.026
Na	0.000	0.001	0.000	0.001	0.000
K	0.000	0.000	0.001	0.001	0.000
Wo	0.8	1.1	1.0	1.3	1.3
En	90.6	90.2	90.5	90.2	90.2
Fs	8.6	8.6	8.5	8.5	8.4

See text for analytical details. Atomic proportions have been calculated on the basis of 6 oxygens.

In general, the chemical compositions of chromites from harzburgites, dunites and chromitites display high amounts of X_{Cr}, X_{Mg}, Al_2O_3 and Cr_2O_3 and low amounts of TiO_2 and Fe_2O_3, and are compositionally similar to podiform Alpine-type chromitites (Bonavia et al., 1993; Leblanc and Nicolas, 1992; Jan and Windley, 1990).

DISCUSSION

The Hajiabad-Esfandagheh Mélange Zone in the Janatabad region includes mantle peridotites consisting mainly of residual harzburgites with lenses of chromitite and their dunite envelopes. We discuss the origin of (1) harzburgites, (2) dunites, and (3) chromitites separately in the following chapter.

Origin of harzburgites

The olivine compositions of harzburgites are similar to those from residual peridotites reported from other ophiolites and orogenic massifs (Fig. 4a, b) (e.g., Arai, 1994). Fig. 4a displays the relationship between Cr-number of chromite and Fo content of the coexisting olivine (Tamura and Arai, 2006). The averaged mineral compositions in harzburgites fall within the olivine-spinel mantle array (OSMA), representing the compositional field of mantle-derived spinel peridotite (Arai, 1994). These samples plot in the fore-arc peridotite field.

The orthopyroxene compositions in harzburgites are depleted in incompatible elements such as Al_2O_3 and TiO_2, in agreement with a high degree of melt extraction. Fig. 5 displays the correlations between Al_2O_3 content of the orthopyroxene and Cr-number of the coexisting chromite (Morishita et al., 2011a). In this diagram, the compositions of harzburgite orthopyroxenes are similar to those from depleted mid-ocean ridge peridotites, such as the Garrett and Hess Deep, East Pacific Rise, as well as to fore-arc ones, such as the Izu-Bonin-Mariana fore-arc peridotites.

Fig. 6a illustrates the compositional relationship between Cr-number and Mg-number of chromites (Morishita et al., 2011a), which straddle the field of mid-ocean ridge and arc peridotites.

The chromites also have low TiO_2 contents (< 0.3 wt%), suggesting a depleted mantle source (Jan and Windley, 1990). Fig. 6b shows the compositional relationship between TiO_2 and Al_2O_3 of chromites (Kamenetsky et al., 2001). On the basis of this diagram, the investigated chromite minerals in harzburgites are consistent with those of mid-ocean ridge peridotites.

In summary, the major element mineral chemistry of the Janatabad harzburgites is consistent with residues after high degree of partial melting.

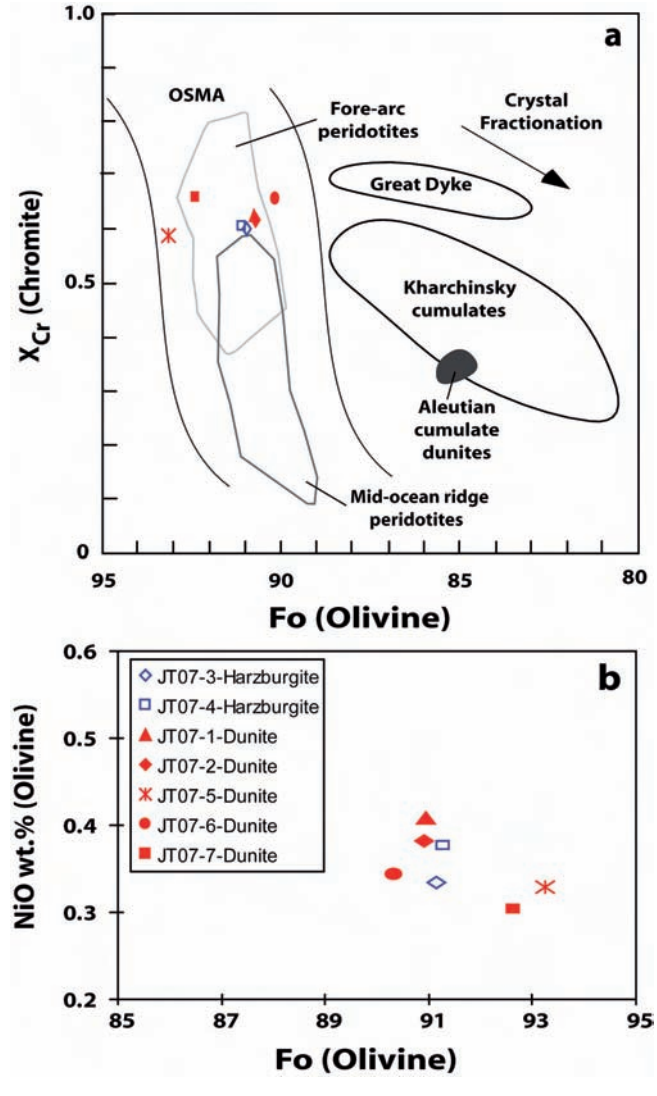

Fig. 4 - (a) Relationships between Cr-number of chromite and Fo content of coexisting olivine in harzburgites and dunites (Tamura and Arai, 2006). The Olivine-Spinel Mantle Array (OSMA) is from Arai (1994) and the Crystal Fractionation trend is from Dick and Bullen (1984). Compositional fields outline for mid-ocean ridge peridotites (Dick and Bullen, 1984), fore-arc peridotites from the Mariana Trench and from the Tonga Trench (Bloomer and Hawkins, 1983; Bloomer and Fisher, 1987), Kharchinsky cumulates (Dektor, 2006), Aleutians cumulate dunites (Debari et al., 1987), and Great Dyke (Wilson, 1982). (b) Variation of NiO (wt%) versus Fo content of olivine in harzburgites and dunites.

Table 3 - Compositions of chromite in harzburgites, dunites and chromitites from the Janatabad peridotites (*continues*).

Sample Rock	JT07-3 Harzburgite	JT07-3 Harzburgite	JT07-3 Harzburgite	JT07-3 Harzburgite	JT07-4 Harzburgite	JT07-4 Harzburgite	JT07-4 Harzburgite	JT07-4 Harzburgite
SiO_2	0.03	0.02	0.04	0.01	0.01	0.02	0.02	0.02
TiO_2	0.30	0.20	0.16	0.26	0.17	0.20	0.20	0.16
Al_2O_3	20.94	21.18	21.03	20.79	20.89	21.02	21.08	21.29
Cr_2O_3	47.07	47.93	46.90	47.61	47.44	48.16	47.35	46.56
Fe_2O_3	1.60	1.20	2.10	2.10	1.74	1.09	1.25	1.82
FeO	16.10	16.60	16.20	16.30	17.92	18.43	18.11	17.93
MnO	0.15	0.27	0.22	0.28	0.37	0.41	0.13	0.32
MgO	12.35	12.13	12.27	12.35	11.15	11.01	11.18	11.16
CaO	0.03	0.03	0.00	0.02	0.06	0.01	0.02	0.01
Total	98.56	99.56	98.91	99.70	99.74	100.35	99.33	99.26
Si	0.007	0.006	0.011	0.001	0.003	0.006	0.005	0.006
Ti	0.057	0.038	0.029	0.049	0.031	0.037	0.037	0.030
Al	6.200	6.223	6.208	6.101	6.174	6.187	6.247	6.306
Cr	9.351	9.448	9.290	9.371	9.406	9.507	9.414	9.253
$Fe^{(3+)}$	0.322	0.242	0.421	0.428	0.353	0.220	0.254	0.370
$Fe^{(2+)}$	3.397	3.470	3.413	3.403	3.771	3.856	3.817	3.782
Mn	0.032	0.056	0.046	0.058	0.079	0.087	0.027	0.067
Mg	4.627	4.509	4.581	4.584	4.169	4.098	4.193	4.183
Ca	0.007	0.009	0.001	0.005	0.015	0.002	0.005	0.003
X_{Cr}	0.60	0.60	0.60	0.61	0.60	0.61	0.60	0.59
X_{Mg}	0.58	0.57	0.57	0.57	0.53	0.52	0.52	0.53
X_{Fe}	0.42	0.43	0.43	0.43	0.47	0.48	0.48	0.47

Sample Rock	JT07-1 Dunite	JT07-1 Dunite	JT07-1 Dunite	JT07-1 Dunite	JT07-2 Dunite	JT07-2 Dunite	JT07-2 Dunite	JT07-2 Dunite	JT07-2 Dunite	JT07-5 Dunite	JT07-5 Dunite
SiO_2	0.02	0.01	0.01	0.05	0.04	0.02	0.03	0.02	0.05	0.04	0.00
TiO_2	0.34	0.35	0.38	0.25	0.25	0.38	0.38	0.35	0.32	0.29	0.27
Al_2O_3	18.21	18.49	18.39	18.40	19.24	18.75	19.56	19.20	19.15	21.04	21.11
Cr_2O_3	46.76	46.04	45.96	46.24	46.06	45.99	45.21	45.38	45.04	43.79	44.95
Fe_2O_3	4.41	4.50	4.20	4.31	3.70	4.41	3.92	3.96	4.47	4.05	2.97
FeO	19.56	20.09	19.48	19.37	19.09	19.16	19.48	18.49	18.66	17.72	17.93
MnO	0.27	0.17	0.15	0.22	0.23	0.36	0.21	0.29	0.21	0.00	0.00
MgO	9.94	9.65	9.87	9.92	10.21	10.15	10.07	10.47	10.44	11.33	11.23
CaO	0.03	0.01	0.03	0.04	0.02	0.03	0.01	0.00	0.01	0.04	0.00
Total	99.54	99.30	98.46	98.79	98.83	99.25	98.87	98.17	98.35	98.30	98.46
Si	0.006	0.004	0.002	0.013	0.011	0.005	0.008	0.006	0.014	0.009	0.000
Ti	0.065	0.067	0.073	0.048	0.048	0.073	0.073	0.068	0.062	0.056	0.052
Al	5.490	5.591	5.595	5.577	5.800	5.645	5.892	5.813	5.789	6.276	6.296
Cr	9.457	9.336	9.380	9.406	9.317	9.289	9.138	9.217	9.135	8.765	8.993
$Fe^{(3+)}$	0.911	0.932	0.875	0.896	0.765	0.911	0.809	0.823	0.926	0.828	0.607
$Fe^{(2+)}$	4.214	4.342	4.236	4.198	4.112	4.124	4.193	4.000	4.035	3.780	3.816
Mn	0.058	0.036	0.033	0.048	0.050	0.079	0.046	0.064	0.045	0.000	0.000
Mg	3.790	3.690	3.799	3.803	3.893	3.866	3.838	4.009	3.993	4.275	4.236
Ca	0.009	0.001	0.007	0.011	0.005	0.008	0.002	0.000	0.002	0.010	0.000
X_{Cr}	0.63	0.63	0.63	0.63	0.62	0.62	0.61	0.61	0.61	0.58	0.59
X_{Mg}	0.47	0.46	0.47	0.48	0.49	0.48	0.48	0.50	0.50	0.53	0.53
X_{Fe}	0.53	0.54	0.53	0.52	0.51	0.52	0.52	0.50	0.50	0.47	0.47

See text for analytical details. Atomic proportions have been calculated on the basis of 32 oxygens.

Origin of dunites

In the plot of Cr-number in chromite versus Fo content in coexisting olivine (Fig. 4a), the averaged mineral compositions of dunites are refractory compared to mid-ocean ridge peridotites and more similar to those reported for fore-arc peridotites from the Mariana and Tonga Trenches.

Chemical analyses of chromites in the dunites are also plotted on the Cr-number versus Mg-number diagram (Fig. 6a). Type 1 dunites plot to the highest end of mid-ocean ridge peridotite field. On the other hand, Type 2 dunites fall in the field of fore-arc peridotites; they also have distinctly lower X_{Cr} than the chromites from boninite-like magmas. On the basis of the TiO_2 versus Al_2O_3 diagram (Fig. 6b),

Table 3 (*continued*)

Sample Rock	JT07-5 Dunite	JT07-5 Dunite	JT07-5 Dunite	JT07-6 Dunite	JT07-6 Dunite	JT07-6 Dunite	JT07-6 Dunite	JT07-7 Dunite	JT07-7 Dunite	JT07-7 Dunite	JT07-7 Dunite
SiO_2	0.11	0.00	0.00	0.02	0.00	0.00	0.00	0.01	0.00	0.06	0.07
TiO_2	0.27	0.25	0.24	0.21	0.21	0.25	0.21	0.21	0.20	0.16	0.23
Al_2O_3	21.43	21.93	21.40	15.62	15.73	15.38	15.62	15.27	15.42	15.48	15.06
Cr_2O_3	44.01	44.98	44.10	45.05	45.86	44.93	45.61	42.82	45.37	44.78	44.68
Fe_2O_3	3.37	3.48	4.77	8.69	8.28	9.53	8.33	9.46	8.67	8.31	8.19
FeO	18.82	19.00	18.75	20.64	21.23	20.99	21.92	21.12	20.99	20.74	21.36
MnO	0.00	0.00	0.00	0.00	0.00	0.00	0.00	0.49	0.68	0.44	0.38
MgO	10.85	11.00	11.07	8.94	8.76	8.82	8.29	7.88	8.35	8.45	7.98
CaO	0.01	0.10	0.01	0.03	0.01	0.08	0.00	0.00	0.00	0.00	0.04
Total	98.88	100.74	100.33	99.19	100.08	99.98	99.98	97.27	99.68	98.41	98.00
Si	0.029	0.000	0.000	0.004	0.000	0.000	0.001	0.003	0.000	0.015	0.019
Ti	0.052	0.047	0.044	0.041	0.041	0.050	0.041	0.042	0.040	0.032	0.047
Al	6.374	6.402	6.277	4.797	4.798	4.697	4.789	4.813	4.739	4.807	4.719
Cr	8.779	8.808	8.676	9.283	9.388	9.207	9.378	9.052	9.354	9.329	9.389
$Fe^{(3+)}$	0.687	0.696	0.959	1.830	1.732	1.997	1.751	2.044	1.827	1.770	1.760
$Fe^{(2+)}$	3.995	3.960	3.936	4.563	4.657	4.618	4.828	4.793	4.642	4.631	4.808
Mn	0.000	0.000	0.000	0.000	0.000	0.000	0.000	0.112	0.150	0.098	0.085
Mg	4.081	4.061	4.106	3.474	3.382	3.408	3.213	3.141	3.247	3.318	3.162
Ca	0.004	0.026	0.003	0.008	0.002	0.023	0.000	0.000	0.001	0.000	0.011
X_{Cr}	0.58	0.58	0.58	0.66	0.66	0.66	0.66	0.65	0.66	0.66	0.67
X_{Mg}	0.51	0.51	0.51	0.43	0.42	0.42	0.40	0.40	0.41	0.42	0.40
X_{Fe}	0.49	0.49	0.49	0.57	0.58	0.58	0.60	0.60	0.59	0.58	0.60

Sample Rock	JT07-8 Chromitite	JT07-8 Chromitite	JT07-9 Chromitite	JT07-9 Chromitite	JT07-9 Chromitite	JT07-9 Chromitite	JT07-10 Chromitite	JT07-10 Chromitite	JT07-10 Chromitite	JT07-10 Chromitite	JT07-10 Chromitite
SiO_2	0.04	0.03	0.00	0.00	0.00	0.00	0.02	0.03	0.01	0.05	0.03
TiO_2	0.32	0.30	0.32	0.30	0.32	0.32	0.34	0.36	0.30	0.30	0.31
Al_2O_3	24.23	24.20	24.30	24.26	23.90	24.19	23.95	24.12	23.87	24.12	23.80
Cr_2O_3	41.96	41.59	42.51	42.79	41.83	42.61	41.81	41.73	42.15	42.31	41.89
Fe_2O_3	3.74	4.43	3.76	3.24	4.34	3.63	3.96	4.47	4.15	3.50	4.49
FeO	12.11	11.85	12.27	12.36	11.83	11.82	12.18	11.51	11.53	11.98	11.37
MnO	0.00	0.00	0.00	0.00	0.00	0.00	0.00	0.00	0.00	0.00	0.00
MgO	15.22	15.41	15.26	15.12	15.32	15.47	15.08	15.68	15.50	15.27	15.61
CaO	0.00	0.00	0.02	0.00	0.00	0.00	0.00	0.00	0.01	0.00	0.00
Total	97.62	97.82	98.44	98.06	97.56	98.04	97.34	97.90	97.52	97.52	97.49
Si	0.010	0.007	0.000	0.000	0.000	0.000	0.004	0.008	0.002	0.012	0.006
Ti	0.059	0.056	0.059	0.054	0.059	0.059	0.063	0.066	0.055	0.054	0.056
Al	6.995	6.968	6.967	6.986	6.909	6.953	6.946	6.929	6.895	6.970	6.871
Cr	8.128	8.033	8.175	8.267	8.112	8.215	8.134	8.042	8.168	8.204	8.114
$Fe^{(3+)}$	0.739	0.874	0.739	0.639	0.860	0.715	0.787	0.880	0.822	0.694	0.889
$Fe^{(2+)}$	2.508	2.451	2.521	2.548	2.456	2.436	2.534	2.377	2.392	2.481	2.360
Mn	0.000	0.000	0.000	0.000	0.000	0.000	0.000	0.000	0.000	0.000	0.000
Mg	5.561	5.611	5.533	5.506	5.602	5.623	5.532	5.697	5.662	5.585	5.703
Ca	0.000	0.000	0.005	0.000	0.001	0.000	0.000	0.000	0.003	0.000	0.000
X_{Cr}	0.54	0.54	0.54	0.54	0.54	0.54	0.54	0.54	0.54	0.54	0.54
X_{Mg}	0.69	0.70	0.69	0.68	0.70	0.70	0.69	0.71	0.70	0.69	0.71
X_{Fe}	0.31	0.30	0.31	0.32	0.30	0.30	0.31	0.29	0.30	0.31	0.29

Type 2 dunites have lower Al_2O_3 concentrations than Type 1 dunites, which are consistent with the field of supra-subduction-zone peridotites.

Two distinctive melts are required for the formation of the Janatabad dunites. The melt genetically related to Type 1 dunites could have had a MORB-like composition, whereas Type 2 dunites were most likely related to a liquid with transitional composition between MORB and boninite.

Field evidence indicates that the Type 1 and Type 2 dunites occur close to each other, and are associated with refractory harzburgites. The boundaries between the dunite envelopes and the harzburgites are relatively sharp, suggesting a replacive origin for these dunites (e.g., Morishita et al., 2011a).

Crystal fractionation would drive cumulate dunites toward low forsterite and NiO values in olivine, and low X_{Cr} in chromite (Dick and Bullen, 1984), whereas dunites are refractory mantle samples that fall within the olivine-spinel mantle array (Fig. 4a). This feature is clearly in contrast to the trend of Fe-enrichment produced during olivine fractionation and observed in nearly all cumulates recognized in ultramafic complexes and in xenoliths (e.g., Wilson, 1982; De Bari et al., 1987; Dektor, 2006).

In contrast, partial melting will drive residual peridotites

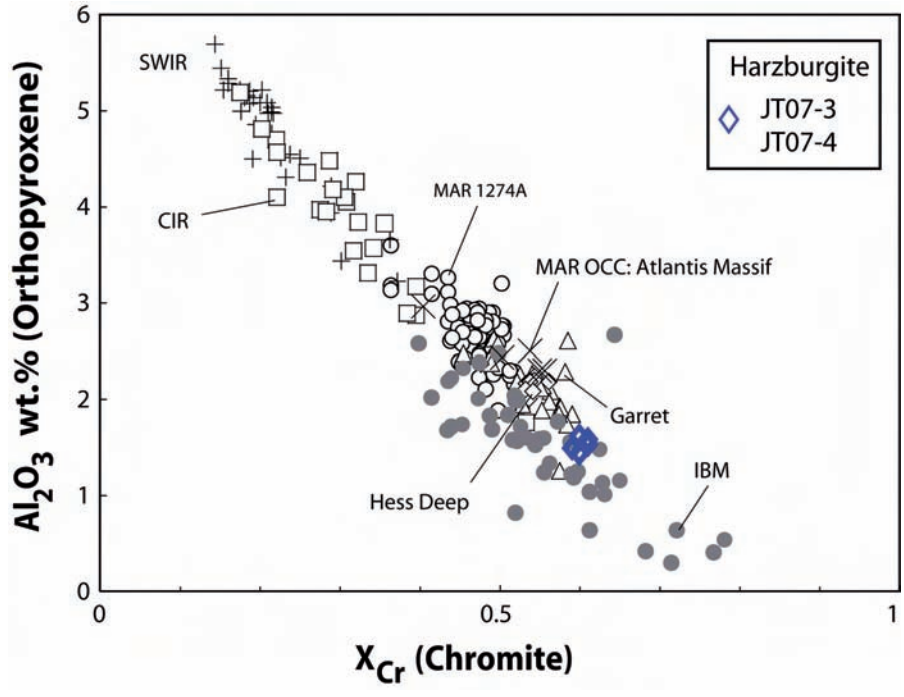

Fig. 5 - Relationship between Al_2O_3 of orthopyroxene and Cr-number of the coexisting chromite in harzburgites (Morishita et al., 2011a). Data sources for the Izu-Bonin-Mariana fore-arc (IBM) (Parkinson and Pearce, 1998; Zanetti et al., 2006), Southwest Indian Ridge (SWIR) (Dick, 1989; Seyler et al., 2003), Central Indian Ridge (CIR) (Hellebrand et al., 2002; Morishita et al., 2009), Mid-Atlantic Ridge (MAR 1274A), Atlantis Massif: Oceanic Core Complex (OCC) (Seyler et al., 2007; Tamura et al., 2008), Garrett and Hess Deep, East Pacific Rise (Dick and Natland, 1996; Constantin, 1999).

toward high forsterite and NiO contents in olivine, and high X_{Cr} in chromite (Dick and Bullen, 1984; Kubo, 2002). Experimental studies show that residual dunites formed by 50% melting would have olivine with Fo_{95} and chromite with X_{Cr} of 80 (Jaques and Green, 1980). In the dunites, olivines have lower amounts of NiO and forsterite compositions (Fig. 4b).

Field and mineral chemistry studies therefore rule out an origin for the dunites either by melt extraction or crystal fractionation. Having ruled out residual mantle or cumulate origins, we will take into account a melt-rock reaction process (Morishita et al., 2011a).

According to several authors (Kelemen and Dick, 1995; Kelemen, 1990; Kelemen et al., 1992; Edwards and Malpas, 1995; Dick and Natland, 1996;), dunites in the mantle section of many ophiolites can form by interaction between infiltrating basaltic melts and upper mantle peridotites, a process that dissolves pyroxene and precipitates olivine. The Janatabad dunites can be therefore products of the interaction between MORB- to transitional-like melts and pre-existing refractory harzburgites.

Origin of chromitites

Typically, chromites in podiform chromitites exhibit a wide range of Cr-number from high-Cr to high-Al in the upper mantle. Cr-rich chromitites have X_{Cr} greater than 0.6, whereas Al-rich chromitites typically have X_{Cr} between 0.4 and 0.6 (Leblanc and Violette, 1983; Zhou and Bai, 1992).

As indicated by the Cr-number versus Mg-number plot (Fig. 5a), chromites mostly fall in the field of mid-ocean ridge peridotites. Therefore, the Janatabad chromitites likely crystallized from MORB-like melts.

The occurrence of dunite envelopes around the podiform chromitites indicates a genetic relationship between them. According to Robinson et al. (1997), dissolution of orthopyroxene and olivine precipitation by a pyroxene-saturated melt may finally lead to silica enrichment in the melt promoting chromite crystallization and formation of chromitite ore bodies. We suggest, therefore, that the interaction between primitive MORB-like melts and depleted harzburgites would have produced secondary silica enriched melts from which Al-rich chromitites crystallized.

Geodynamic implications

According to the subduction infancy model (Stern and Bloomer, 1992; Stern, 2004; Stern et al., 2012), subsidence of old lithosphere allows asthenosphere to flood over it. Because of decompression melting, the upwelling asthenosphere (mid-ocean ridge peridotites) generates early proto-fore-arc spreading (MORB-like melts) accompanied by seafloor spreading in the extensional region. Continued subsidence of lithosphere is accompanied by penetration of slab-derived fluids into the overlying mantle wedge, causing formation of refractory peridotites (fore-arc peridotites) and generates late proto-fore-arc spreading (VAB-BON-like melts).

Reagan et al. (2010) indicated that MORB-like basalts termed as fore-arc basalts (FAB) are overlain by transitional lava and boninites in the Izu-Bonin-Mariana fore-arc. The most likely origin of fore-arc basalts is that they were the first lavas erupted during near-trench spreading after subduction began. The presence of transitional lavas with compositions between MORB and boninites indicates that fluids from the sinking lithosphere become increasingly important with time in subduction related environments. The most likely origin of transitional lavas and boninites is that they were generated later when the residual mantle melted at shallow levels after being fluxed by a water-rich fluid derived from the sinking plate.

The Janatabad harzburgites are very similar to strongly depleted mid-ocean ridge peridotites (Figs. 3, 4 and 5), indicating an origin as residue after high degree of partial melting and MORB-like magma extraction (fore-arc basalt of Reagan et al., 2010), most likely during the earliest stages of subduction.

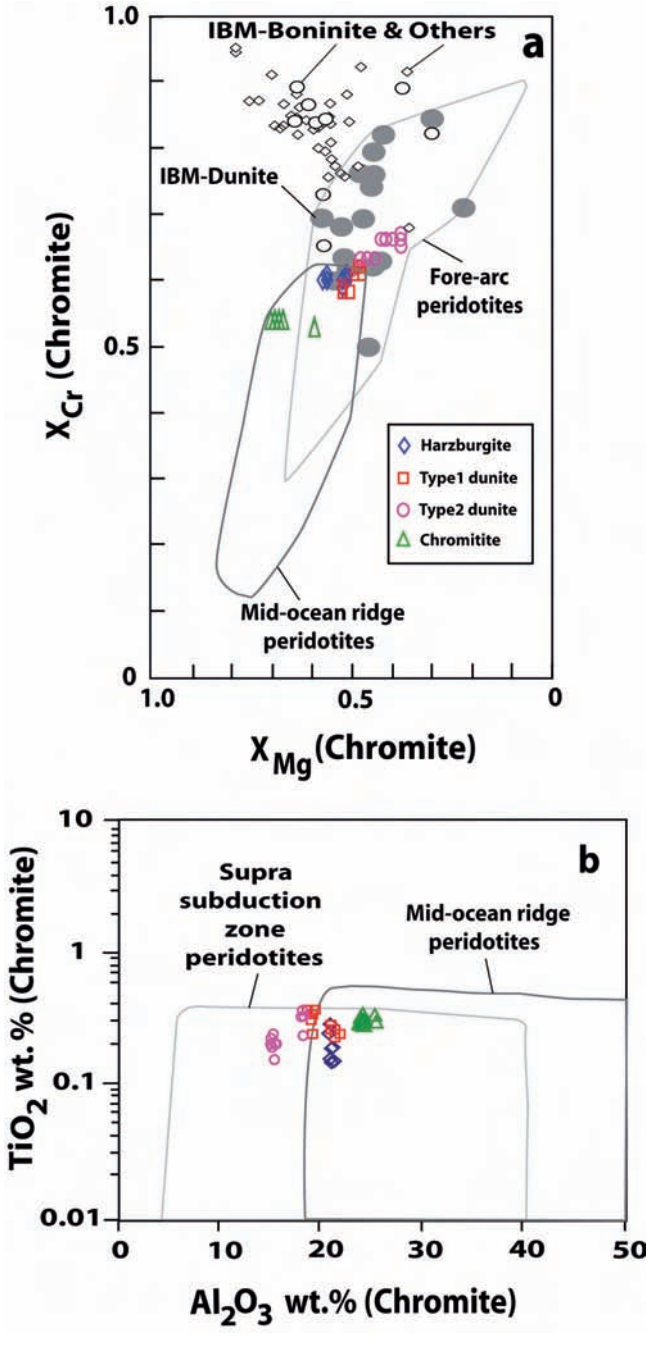

Fig. 6 - (a) Relationship between Cr-number and Mg-number of chromite in harzburgites, dunites and chromitites (Morishita et al., 2011a). Compositional fields outline for mid-ocean ridge peridotites (Dick, 1989; Arai and Matsukage, 1998; Constantin, 1999; Hellebrand et al., 2002; Seyler et al., 2003) and fore-arc peridotites (Ishii et al., 1992; Parkinson and Pearce, 1998). The averaged data for the Izu-Bonin-Mariana dunite (IBM-Dunite) (Ishii et al., 1992), Izu-Bonin-Mariana boninites (IBM-Boninites) and other localities (Others) (Kuroda et al., 1978; Walker and Cameron, 1983; Bloomer and Hawkins, 1987; Falloon et al., 1989; Van der Laan et al., 1992; Sobolev and Danyushevsky, 1994). (b) Variation of Al_2O_3 (wt%) versus TiO_2 (wt%) of chromite in harzburgites, dunites and chromitites (Kamenetsky et al., 2001).

Type 1 dunites may have a genetic link to MORB-like melts. In contrast, Type 2 dunites may have genetic link to transitional-like melts with composition between MORB- and boninite-like melts (Figs. 3 and 5). The geochemical features of dunites, may be therefore be related to the increasing contribution of subduction-related components to the overlying mantle wedge at the beginning of the down-dip motion of the slab. Such mantle peridotites commonly originate in fore-arc basins as subduction begins (e.g., Morishita et al., 2011b).

The primitive MORB- to transitional-like melts react with the depleted harzburgites and dissolve pyroxene from the wall rock. Such interaction would increase the silica content of the melts and lead to crystallization of Al-rich chromitites.

CONCLUDING REMARKS

The subject of the present work covers the Janatabad peridotites that are exposed in the Hajiabad-Esfandagheh Mélange Zone in southern Iran. Harzburgites include small lenses and veins of chromitite pods surrounded by dunite envelopes. Accordingly, harzburgites, dunites and chromitites indicate three stages of magma generation in the Janatabad peridotites. At the first stage, the depleted harzburgites originate as the residue after high degree of partial melting and MORB-like magma extraction during the earliest stage of subduction. At the second stage, the interaction between primitive MORB-like melts and depleted harzburgites produced Type 1 dunites and secondary silica-rich melts from which Al-rich chromitites crystallized. A third stage of melting at depth produced Type 2 dunites by interaction between transitional-like melts and depleted harzburgites above a lithosphere in continuous subsidence. These compositional variations from MORB- to transitional-like melts are due to the hydrous fluids derived from the subducted oceanic slab into the overlying mantle wedge. Therefore, in our preferred scenario the Janatabad peridotites formed by rifting of a Late Triassic to Early Jurassic embryonic ocean during subduction initiation of the Neo-Tethyan lithosphere in an intra-oceanic environment.

ACKNOWLEDGMENTS

This study was financially supported by the Islamic Azad University, Estahban Branch, and by French CNRS, the Cultural Service of the French Embassy at Tehran. Michel Fialin and Frédéric Couffignal (Service CAMPARIS Campus Universitaire Jussieu, Paris) are thanked for their patience and persistence in undertaking the mineral analyses. The authors are greatly indebted to the editors of Ofioliti, Professor Riccardo Tribuzio and Professor Alessandra Montanini for greatly helping in this research. Finally, the authors are very grateful to reviewers of Ofioliti, Professor Emilio Saccani and especially Professor Tomoaki Morishita for their fruitful discussions, precise revisions and valuable comments concerning the manuscript.

REFERENCES

Ahmadipour H., Sabzehi M., Whitechurch H., Rastad E. and Emami M.H., 2003. Soghan complex as an evidence for paleospreading center and mantle diapirism in Sanandaj-Sirjan zone (south-east Iran). J.Sci., Islamic Republic Iran, 14 (2): 157-172.

Arai S., 1994. Characterization of spinel peridotites by olivine-spinel compositional relationships: review and interpretation. Chem. Geol., 113: 191-204.

Arai S., Kodoshima K. and Morishita K., 2006. Widespread arc-related melting in the mantle section of the northern Oman ophiolite as inferred from detrial chromian spinels. J. Geol. Soc., 163: 869-879.

Arai S. and Matsukage K., 1998. Petrology of a chromitite micropod from Hess Deep, equatorial Pacific: a comparison between abyssal and alpine-type podiform chromitites. Lithos, 43: 1-14.

Azizan H. and Nazemzadeh A., 2006. Geological map of the Orzuieh, Scale 1/100,000. Geol. Surv. Iran, Sheet 7246.

Barnes S.J. and Roeder P.L., 2001. The range of spinel composition in terrestrial mafic ultramafic rocks. J. Petrol., 42: 2279-2302.

Berberian M. and King G.C.P., 1981. Towards a paleogeography and tectonic evolution of Iran. Can. J. Earth Sci., 18: 210-265.

Bloomer S.H. and Fisher R.L., 1987. Petrology and geochemistry of igneous rocks from the Tonga Trench - a non-accreting plate boundary. J. Geol., 95: 469-495.

Bloomer S.H. and Hawkins J.W., 1983. Gabbroic and ultramafic rocks from the Mariana trench: an island arc ophiolite. In: D.E. Hayes (Ed.), The tectonics and geologic evolution of southeast Asian seas and islands: Part II. Am. Geophys. Union, Washington, p. 294-317.

Bloomer S.H. and Hawkins J.W., 1987. Petrology and geochemistry of boninite series volcanic rocks from the Mariana trench. Contrib. Mineral. Petrol., 97: 361-377.

Bonavia F.F., Diella V. and Ferrario A., 1993. Precambrian podiform chromitites from Kenticha Hill, southern Ethiopia. Econ. Geol., 88: 198-202.

Constantin M., 1999. Gabbroic intrusions and magmatic metasomatism in harzburgites from the Garrett transform fault: implications for the nature of the mantle-crust transition at fast-spreading ridges. Contrib. Mineral. Petrol., 136: 111-130.

De Bari S., Mahlburg Kay S., and Kay R.W., 1987. Ultramafic xenoliths from Adagdak volcano, Adak, Aleutian Islands, Alaska: Deformed igneous cumulates from the Moho of an island arc. J. Geol., 95: 329-341.

Dektor C., 2006. Petrology and geochemistry of mafic and ultramafic xenoliths from Kharchinsky volcano, Kamchatka. Univ. South Carolina. Master's thesis, 75 pp.

Dick H.J.B., 1989. Abyssal peridotites, very slow spreading ridges and ocean ridge magmatism. In: A.D. Saunders and M.J. Norry (Eds.), Magmatism in the ocean basins, Geol. Soc. London Spec. Publ., 42: 71-105.

Dick H.J.B. and Bullen T., 1984. Chromian spinel as a petrogenetic indicator in abyssal and alpine-type peridotites and spatially associated lavas. Contrib. Mineral. Petrol., 86: 54-76.

Dick H.J.B. and Natland J.H., 1996. Late-stage melt evolution and transport in shallow mantle beneath the East Pacific Rise. In: C. Mével, K.M. Gillis and F. Allan (Eds.), Proceed. O.D.P. Sci. Results, 147: 103-134.

Edwards S.J. and Malpas J., 1995. Multiple origins for mantle arzburgites: examples from the Lewis Hills massif, Bay of Islands ophiolite, Newfoundland. Can. J. Earth Sci., 32: 1046-1057.

Falloon T.J., Green D.H. and McCulloch M.T., 1989. Petrogenesis of high-Mg and associated lavas from the north Tonga Trench. In: A.J. Crawford (Ed.), Boninites and related rocks. Unwin Hyman Ltd., p. 357-395.

Ghasemi H., Juteau T., Bellon H., Sabzehi M., Whitechurch H. and Ricou L.E., 2002. The mafic-ultramafic complex of Sikhoran (central Iran): a polygenetic ophiolite complex. C. R. Geosci., 334: 431-438.

Hellebrand E., Snow J.E., Dick H.J.B. and Hofmann A.W., 2002. Garnet-field melting and later-stage refertilizaiton in 'residual' abyssal peridotites from the central Indian Ridge. J. Petrol., 43: 2305-2338.

Ishii T., Robinson P.T., Maekawa H. and Fiske R., 1992. Petrological studies of peridotites from diapiric serpentinite seamounts in The Izu-Ogasawara-Mariana forearc, LEG125. In: P. Fryer, J.A. Pearce and L.B. Stokking (Eds.), LEG 125 Proc. ODP Sci. Results, 125: 445-485.

Jan M.Q. and Windley B.F., 1990. Chromian spinel-silicate chemistry in ultramafic rocks of the Jijal complex, Northwest Pakistan. J. Petrol., 31: 667-715.

Jaques A.L., and Green D.H., 1980. Anhydrous melting of peridotite at 0-15 Kb pressure and the genesis of tholeiitic basalts. Contrib. Mineral. Petrol., 73: 287-310.

Kamenetsky V., Crawford A. and Meffre S., 2001. Factors controlling chemistry of magmatic spinel: an empirical study of associated olivine, Cr-spinel and melt inclusions from primitive rocks. J. Petrol., 42: 655-671.

Kelemen P.B., 1990. Reaction between ultramafic rock and fractionating basaltic magma I. Phase relations, the origin of calc-alkaline magma series, and the formation of discordant dunite. J. Petrol., 31: 51-98.

Kelemen P.B. and Dick. J.B., 1995. Focused melt flow and localized deformation in the upper mantle: juxtaposition of replacive dunite and ductile shear zones in the Josephine peridotites, SW Oregon. J. Geophys. Res., 100 (B1): 423-438.

Kelemen P.B., Dick H.J.B. and Quick J.E., 1992. Formation of harzburgite by pervasive melt/rock reaction in the upper mantle. Nature, 358: 635-641.

Kubo K., 2002. Dunite formation processes in highly depleted peridotite: case study of the Iwanaidake peridotite, Hokkaido, Japan. J. Petrol., 43: 423-448.

Kuroda N., Shiraki K. and Urano H., 1978. Boninite as a possible calc-alkalic primary magma. Bull. Volcan., 41: 563-575.

Leblanc M. and Nicolas A., 1992. Les chromitites ophiolitiques. Chron. Recher. Min., 507: 3-25.

Leblanc M. and Violette J.F., 1983. Distribution of AI-rich and Cr-rich chromite pods in ophiolites. Econ. Geol., 78: 293-301.

Morishita T., Dilek Y., Shallo M., Tamura A. and Arai S., 2011a. Insights into the uppermost mantle section of a maturing arc: The eastern Mirdita ophiolite, Albania. Lithos, 124: 215-226.

Morishita T., Hara K., Nakamura K., Sawaguchi T., Tamura A., Arai S., Okino K., Takai K. and Kumagai H., 2009. Igneous, alteration and exhumation processes recorded in abyssal peridotites and related fault rocks from an oceanic core complex along the Central Indian Ridge. J. Petrol., 50: 1299-1325.

Morishita T., Tani K., Shukuno H., Harigane Y., Tamura A., Kumagai H. and Hellebrand E., 2011b. Diversity of melt conduits in the Izu-Bonin-Mariana forearc mantle: implications for the earliest stage of arc magmatism. Geology, 39 (4): 411-414.

Parkinson I.J. and Pearce J.A., 1998. Peridotites from the Izu-Bonin-Mariana forearc (ODP Leg 125): evidence for mantle melting and melt-mantle interaction in a supra-subduction zone setting. J. Petrol., 39: 1577-1618.

Pearce J.A., Barker P.F., Edwards S.J., Parkinson I.J. and Leat P.T., 2000. Geochemistry and tectonic significance of peridotites from the South Sandwich arc basin system, South Atlantic. Contrib. Mineral. Petrol., 139: 36-53.

Reagan M.K., Ishizuka O., Stern R.J., Kelley K.A., Ohara Y., Blichert-Toft J., Bloomer S.H., Cash J., Fryer P., Hanan B.B., Hickey-Vargas R., Ishii T., Kimura J.I., Peater D.W., Rowe M.C. and Woods M., 2010. Fore-arc basalts and subduction initiation in the Izu-Bonin-Mariana system. Geochem. Geophys. Geosyst., 11 (3): 1-17.

Robinson P.T., Zhou M.F., Malpas J. and Bai W.J., 1997. Podiform chromitites: their composition, origin and environment of formation. Episodes, 20: 247-252.

Seyler M., Cannat M. and Mével C., 2003. Evidence for major-element heterogeneity in the mantle source of abyssal peridotites from the Southwest Indian Ridge (52° to 68°E). Geochem. Geophys. Geosyst., 4: 9101.

Seyler M., Loarnd J.-P., Dick H.J.B. and Drouin M., 2007. Pervasive melt percolation reactions in ultra-depleted refractory harzburgites at the Mid-Atlantic Ridge, 15° 20□N: ODP Hole 1274A. Contrib. Mineral. Petrol., 153: 303-319.

Stern R.J., 2004. Subduction initiation: Spontaneous and induced. Earth Planet. Sci. Lett., 226: 275-292.

Stern R.J. and Bloomer S.H., 1992. Subduction zone infancy-Examples from the Eocene Izu-Bonin-Mariana and Jurassic California arcs. Geol. Soc. Am. Bull., 104: 1621-1636.

Stern R.J., Reagan M., Ishizuka O., Ohara Y. and Whattam S., 2012. To understand subduction initiation, study forearc crust: To understand forearc crust, study ophiolites. Lithosphere, 4: 469-483.

Sobolev A.V. and Danyushevsky L.V., 1994. Petrology and geochemistry of boninites form the north termination of the Tonga trench: constraints on the generation conditions of primary high-Ca boninite magmas. J. Petrol., 35: 1183-1211.

Tamura A. and Arai S., 2006. Harzburgite-dunite-orthopyroxenite suite as a record of supra-subduction zone setting for the Oman ophiolite mantle. Lithos, 90: 43-56.

Tamura A., Arai S., Ishimaru S. and Andal E.S., 2008. Petrology and geochemistry of peridotites from IODP Site U1309 at Atlantis Massif, MAR 30°N: micro- and macroscale melt penetrations into peridotites. Contrib. Mineral. Petrol., 155: 491-509.

Van der Laan S.R., Arculus R.J., Pearce J.A. and Murton J.B., 1992. Petrography, mineral chemistry, and phase relations of the basement boninite series of Site 786, Izu-Bonin forearc. In: P. Fryer, J.A. Pearce and L.B. Stokking (Eds.), Proceed. O.D.P. Sci. Results, 125: 171-202.

Walker D.A. and Cameron W.E., 1983. Boninite primary magmas: evidence from the Cape Vogel Peninsula, PNG. Contrib. Mineral. Petrol., 83: 150-158.

Wilson A.H., 1982. The geology of the Great Dyke, Zimbabwe: The ultramafic rocks. J. Petrol., 23: 240-292.

Zanetti A., D'Antonio M., Spadea P., Raffone N., Vannucci R. and Brugeir O., 2006. Petrogenesis of mantle peridotites from the Izu-Bonin-Mariana (IBM) forearc. Ofioliti, 31: 189-206.

Zhou M.F. and Bai W.J., 1992. Chromite deposits in China and their origin. Mineral. Dep., 27: 192-199.

Received, March 12, 2012
Accepted, September 12, 2014